CHARACTERIZATION OF LAMB-TYPE WAVES ON A CYLINDRICAL SHELL BY MEANS OF QUALITY FACTORS

PACS REFERENCE: 43.20.Ks

Lenoir Olivier; Conoir Jean-Marc; Izbicki Jean-Louis
LAUE, CNRS UMR 6068 et Université du Havre
Place R. Schuman
76610 LE HAVRE
France
Tel: (33)0232744643
Fax: (33)0232744719
E-mail: lenoir@iut.univ-lehavre.fr

ABSTRACT

We consider the phase of the eigenvalues of the S-matrix associated to a cylindrical evacuated shell immersed in a fluid. The study of the phase partial derivatives with respect to the frequency, the incident angle, the phase velocities of longitudinal and transverse waves in the shell, at a resonance frequency, leads to the introduction of frequency Q_x, angular Q_y, longitudinal Q_L and transverse Q_T quality factors. For shells of b/a=0.8, the wave polarization is analyzed by studying the evolutions of $Q_{L,T}$, in the reduced frequency range 10-250. The evolutions of $Q_{x,y}$ allow to determine the wave energy velocities.

INTRODUCTION

The formalism of the so-called Phase Gradient Method (PGM) was first established by J. M. Conoir [1], in the case of cylindrical shells. It consists in studying the partial derivatives of the eigenphase δ_n of the S matrix associated to the shell. A fundamental relation, which is the basis of the PGM, links the frequency phase derivative to the phase derivatives with respect to the longitudinal and transverse phase velocities of the corresponding waves propagating in the elastic shell and with respect to the phase velocity of the waves propagating in the surrounding fluid. It was shown, in the case of plane geometries, that an analogous relation exists, dealing with the phase of the reflection coefficient of an immersed elastic plate [2]. In this latter case, it is proved that the PGM naturally leads to the introduction of frequency, angular, longitudinal and transverse radiation quality factors. We show in this paper, that these quality factors can also be introduced for cylindrical shells. By analogy with the plate results, we establish that the study of the longitudinal and transverse Q factors allows us to obtain the polarization state of the Lamb-type waves and torsional waves (T waves) propagating in the shell. In addition, the evolutions of the frequency and angular quality factors give the energy velocity of given waves. In a first part, we recall the basis of the PGM applied to cylindrical shells. In a second part, we present the different quality factors. In a third part, the wave polarization state is studied by means of the $Q_{L,T}$ factors. In a fourth part, it is shown that the energy velocity depends on the $Q_{x,y}$ factors.

II BASIS OF THE PHASE GRADIENT METHOD (PGM) APPLIED TO CYLINDRICAL SHELLS

It was shown [1] that the n^{th} eigenvalue S_n, related to the mode number n, of the scattering matrix S, can be written as

$$S_n = -\frac{D_n^*}{D_n} \qquad \text{Eq. (1)}$$

where D_n is the determinant derived from the writing of the boundary conditions. In the case of an evacuated cylindrical shell, D_n is the determinant of a (7×7) matrix and the asterisk * indicates the complex conjugation. As $|S_n| = 1$, we can write

$$S_n = e^{2j\delta_n} \qquad \text{Eq. (2)}$$

where δ_n is the half-eigenphase corresponding to the eigenvalue S_n.

Taking into account an appropriate background (it generally depends on the b/a ratio (a: shell outer radius and b: inner radius)), we can decompose S_n as

$$S_n = S_n^{(bg)}\, S_n^{(*)} \qquad \text{Eq. (3)}$$

where $S_n^{(bg)}$ corresponds to the background part of S_n and $S_n^{(*)}$ to its resonant part.

So, the half-eigenphase δ_n can be written as

$$\delta_n = \delta_n^{(bg)} + \delta_n^{(*)}. \qquad \text{Eq. (4)}$$

In the following we study an evacuated aluminum shell of b/a = 0.8, for which a rigid background is commonly considered as well adapted.

The half-eigenphase δ_n and its components explicitly depend on the frequency f (or the normalized frequency $x = 2\pi f a / c_F$), the phase velocities $c_{L,T}$ of the longitudinal and transverse waves which propagate in the elastic shell, and on the phase velocity c_F of the waves propagating in the surrounding fluid medium, as well as on the incidence angle θ (or its sine y) and the ratio $\rho = \rho_S / \rho_F$ of the density of the shell to that of the fluid. It was demonstrated by J.M. Conoir [1] that the partial derivatives of δ_n, with respect to f, $c_{L,\ T,\ F}$, y and ρ can be obtained thanks to the following formula:

$$\frac{\partial \delta_n}{\partial\ f, x, c_{L,T,F}, y, \rho} = -\mathrm{Im}\left(\frac{\dfrac{\partial D_n}{\partial f,\ x,\ c_{L,T,F}, y, \rho}}{D_n} \right) \qquad \text{Eq. (5)}$$

where Im indicates the imaginary part.

One has:

$$x\frac{\partial \delta_n}{\partial x} = f\frac{\partial \delta_n}{\partial f}. \qquad \text{Eq. (6)}$$

In addition, the following fundamental relation, which is the basis of the PGM has been proved:

$$f\frac{\partial \delta_n}{\partial f} + c_L\frac{\partial \delta_n}{\partial c_L} + c_T\frac{\partial \delta_n}{\partial c_T} + c_F\frac{\partial \delta_n}{\partial c_F} = 0. \qquad \text{Eq. (7a)}$$

As $D_n^{(rig)} = H_n^{(1)'}(x\cos\theta)$, the eigenphase $\delta_n^{(rig)}$ only depends on f, c_F and $y = \sin\theta$. We can show

$$f\frac{\partial \delta_n^{(rig)}}{\partial f} + c_F\frac{\partial \delta_n^{(rig)}}{\partial c_F} = 0. \qquad \text{Eq. (7b)}$$

So, we deduce from the previous equations the following one:

$$x\frac{\partial \delta_n^{(*)}}{\partial x} + c_L\frac{\partial \delta_n^{(*)}}{\partial c_L} + c_T\frac{\partial \delta_n^{(*)}}{\partial c_T} + c_F\frac{\partial \delta_n^{(*)}}{\partial c_F} = 0. \qquad \text{Eq. (8)}$$

This equation is valid whatever the incidence angle and the reduced frequency x, in particular for a resonance frequency x_{Res}. x_{Res} is the real part of a frequency pole of S_n (or a root of D_n), generally denoted as

$$\underline{x}_P = x_{Res} - j\frac{\Gamma}{2} \qquad \text{Eq. (9)}$$

where Γ is the half-width of the associated resonance.

From the Resonant Scattering Theory (RST), we can obtain, in the vicinity of a resonance reduced frequency x_{Res}, the following approximate expression of the frequency resonant phase derivative:

$$\left(x\frac{\partial\delta_n^{(*)}}{\partial x}\right)_{app}(x)=\frac{x_{Res}\frac{\Gamma}{2}}{\left(x-x_{Res}\right)^2+\left(\frac{\Gamma}{2}\right)^2}. \qquad \text{Eq. (10)}$$

When $x = x_{Res}$, one has:

$$\left(x\frac{\partial\delta_n^{(*)}}{\partial x}\right)_{app}(x_{Res})=2\frac{x_{Res}}{\Gamma}. \qquad \text{Eq. (11)}$$

So, the function $x\partial\delta_n^{(*)}/\partial x$, calculated at x_{Res}, is proportional to the classical frequency quality factor defined as the ratio x_{Res}/Γ. In the following, it is denoted as Q_x.

The following numerical results are obtained for an aluminum cylindrical shell immersed in water. The values of the parameters used are: aluminum density $\tilde{n}_S$=2790 kg/m^3, longitudinal phase velocity c_L=6380 m/s, transverse phase velocity c_T=3100 m/s, water density $\tilde{n}_F$=1000 kg/m^3 and wave phase velocity in water c_F=1470 m/s.

In Figure1, we have compared the frequency plots of the exact function $x\partial\delta_n^{(*)}/\partial x$ (solid line) and of its approximate expression $x\partial\delta_{n\,app}^{(*)}/\partial x$ (dashed line), for the mode number n = 1 assigned to the Lamb-type wave A_3, at $\theta=5°$. In these conditions, the exact calculation of the frequency pole give $\underline{x}_{A_3}=145.66-j\,1.73$.

The two curves are well superimposed. Each plot exhibits a Breit-Wigner shape, whose maximum is centered on the resonance frequency x_{Res} and whose maximum amplitude corresponds to the ratio $-Re\left(\underline{x}_{A_3}\right)/Im\left(\underline{x}_{A_3}\right)$.

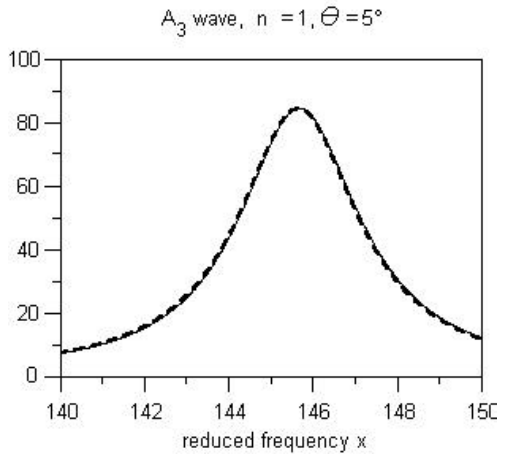

Figure 1: Plots of the exact function $x\frac{\partial\delta_n^{(*)}}{\partial x}$ (solid line) and of the approximate one $\left(x\frac{\partial\delta_n^{(*)}}{\partial x}\right)_{app}$ (dotted line).

The frequency plots of each function $u\partial\delta_n^{(*)}/\partial u,\ u=c_{L,T,F}$, also exhibit Breit-Wigner shapes, as shown in Figure 2. They present extremums, nearly centered on the resonant frequency x_{Res} and their half-widths are the same as the one of the function $x\partial\delta_n^{(*)}/\partial x$.

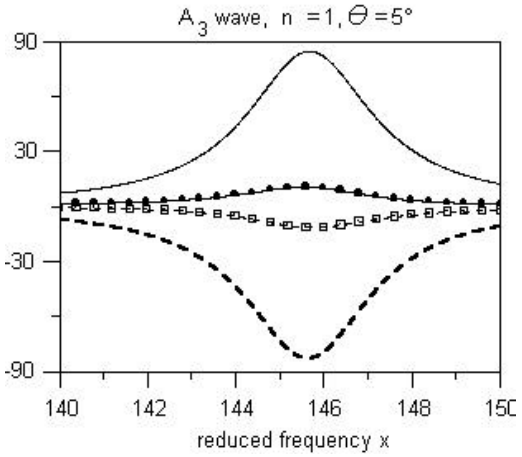

Figure 2: Plots of the functions $x\frac{\partial\delta_n^{(*)}}{\partial x}$ (solid line), $c_L\frac{\partial\delta_n^{(*)}}{\partial c_L}$ (dotted line), $c_T\frac{\partial\delta_n^{(*)}}{\partial c_T}$ (box line) and $c_F\frac{\partial\delta_n^{(*)}}{\partial c_F}$ (filled circle line).

By analogy with the frequency phase derivative, all the functions $u\partial\delta_n^{(*)}/\partial u$, $u=c_{L,T,F}$, calculated at x_{Res}, are also proportional to quality factors. We set

$$\left(c_{L,T,F}\frac{\partial\delta_n^{(*)}}{\partial c_{L,T,F}}\right)(x_{Res}) = 2\varepsilon_{L,T,F}Q_{L,T,F} \qquad \text{Eq. (12)}$$

where $\varepsilon_{L,T}=-1$ and $\varepsilon_F=1$, according to the sign of the associated phase derivative, in the vicinity of x_{Res}. The quality factors $Q_{L,T}$ are qualified as longitudinal and transverse quality factors. For Lamb-type waves on a shell, we can also verify the relation :

$$\left(c_F\frac{\partial\delta_n^{(*)}}{\partial c_F}\right)(x_{Res}) = \left(-y\frac{\partial\delta_n^{(*)}}{\partial y}\right)(x_{Res}). \qquad \text{Eq. (13)}$$

The quality factor Q_F is therefore equal to an angular quality factor, denoted as Q_y.
Written at a resonance frequency x_{Res}, the basis equation of the PGM leads to the following balance

$$Q_x + Q_y = Q_L + Q_T. \qquad \text{Eq. (14)}$$

In the following section, we show the interest to study the evolutions of these quality factors, or ratios depending on them, as in the case of plates.

III VALIDATION FOR CYLINDRICAL SHELLS OF PLATE RESULTS

In the case of plates, we obtain a relation linking the partial derivatives of the phase ϕ of the reflection coefficient $\underline{R}$ of the immersed plate, analog to Eq. (8). The advantage of such a geometry is the fact that there is no need to remove a background. Moreover, the factorized expression of $\underline{R}$ allows us to obtain, in a much simpler way, the phase partial derivatives. We can also easily separate the phase contribution of the symmetric and antisymmetric waves. It can be analytically demonstrated that Q_x is proportional to the spatio-temporal mean energy associated to both longitudinal and transverse standing waves in the thickness of the plate, Q_y to the spatio-temporal mean energy associated to both longitudinal and transverse guided waves along the plate, and $Q_{L,T}$ are respectively proportional to spatio-temporal mean energies associated to the longitudinal and transverse waves propagating in the plate. Therefore, the ratios $Q_x/(Q_x+Q_y)$ and $Q_y/(Q_x+Q_y)$ can be interpreted as a stationary wave ratio (SWR) and a guided wave ratio (GWR). In addition, the ratios $Q_L/(Q_L+Q_T)$ and $Q_T/(Q_L+Q_T)$ can be interpreted respectively as a longitudinal wave ratio (LWR) and a transverse wave ratio (TWR). The study of the evolutions of the ratios $Q_{L,T}/(Q_L+Q_T)$, when the dispersion curve of a given wave is followed, indicates the evolution of the polarization state of this wave. We can immediately

conclude from the plots of those ratios if the wave considered is rather longitudinal or rather transverse. Moreover, it is shown that the energy velocity V_E, which is, in most cases, identical to the group velocity V_G, can be obtained straightforwardly by:

$$V_E = \frac{Q_y}{Q_x + Q_y} V_\varphi \qquad \text{Eq. (15)}$$

where V_φ is the wave phase velocity.

In the following, we verify the validity of these plate results for different Lamb-type waves propagating on the aluminum cylindrical shell, as those shown in Figure 3. In this figure, we have plotted the dispersion curves of antisymmetric modes A_1, A_2 and A_3 (dotted lines) and symmetric modes S_0, S_1, S_2 and S_3 (solid lines), in the reduced frequency range 10-500. The dispersion curves of the torsional waves are also exhibited (bold dashed lines).

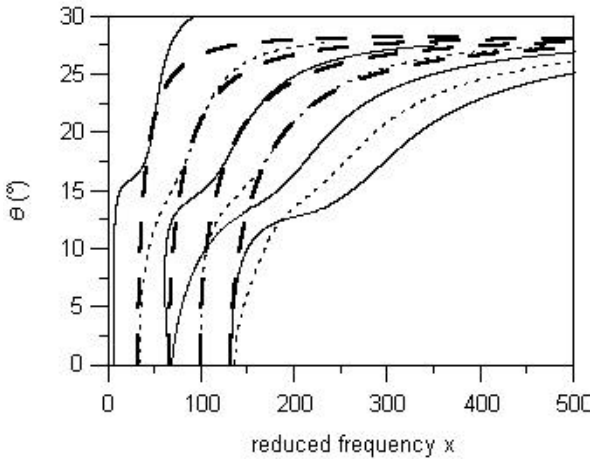

Figure 3: Plots of the dispersion curves of symmetric Lamb-type waves S_0, S_1, S_2 and S_3 (solid lines), of antisymmetric Lamb-type waves A_1, A_2 and A_3 (dotted lines) and of torsional waves (bold dashed lines) (mode number n = 1)

In Figure 4, we have plotted the evolutions of the longitudinal wave ratios $Q_L/(Q_L+Q_T)$ of the different Lamb-type waves, following their dispersion curves. The ratio $Q_L/(Q_L+Q_T)$ ranges from 0 to 1: when it tends to 1, the wave is mainly longitudinal and when it tends to 0, the wave is mainly transverse. Beyond the first critical angle $\theta_C^{(L)} = 13{,}32°$, the longitudinal waves become evanescent, therefore, for all the Lamb-type waves the ratio $Q_L/(Q_L+Q_T)$ tends to 0. By inspection of Figure 4, we can observe that for the modes whose cut-off frequencies are close to a multiple of $c_L/2d$ (longitudinal modes), d being the shell thickness, the ratio $Q_L/(Q_L+Q_T)$ tends to 1, at low incidence angles, as for the S_2 and A_3 modes. Conversely, the modes whose cut-off frequencies are close to a multiple of $c_T/2d$ (transverse modes) have a ratio $Q_L/(Q_L+Q_T)$ which tends to 0, as for the A_1, A_2, S_1 and S_3 modes. When the incidence angle increases, the longitudinal wave ratios evolve according to the polarization state of each wave. We notice that all along their dispersion curves, the A_1 and A_2 modes remain mainly transverse modes and the S_2 mode mainly a longitudinal mode. The mode A_3 becomes progressively a transverse mode. The mode S_3, which is mainly a transverse mode when the incidence angle ranges from 0° to nearly 10°, becomes longitudinal at about 12.5°. We can conclude that the study of the ratio $Q_L/(Q_L+Q_T)$ is well suited to the determination of the polarization state of the Lamb-type waves.

In Figure 5, we have plotted the evolutions of the energy velocities of the different Lamb-type waves, using Eq. (15). When compared to the evolutions of the group velocities, classically obtained by

$$V_G = \frac{\partial \omega}{\partial K_z} \qquad \text{Eq. (16)}$$

where ω is the angular frequency and K_z is the z-component of all the wave vectors involved in the problem (the z-axis is parallel to the cylindrical shell axis), we obtain exactly the same curves. Figure 5 shows the validity of Eq.(15), on the one hand, and the equality of V_E and V_G for the Lamb-type waves studied, on the other hand.

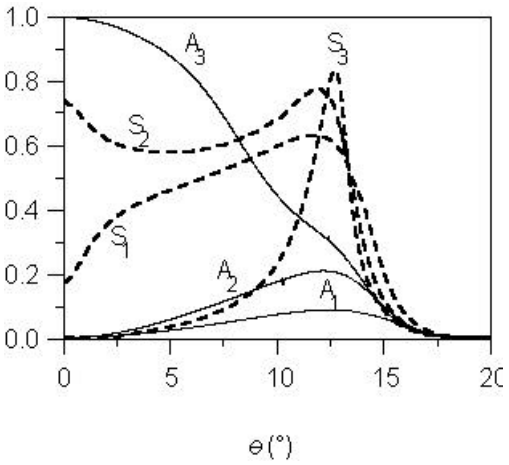

Figure 4: Angular evolutions of the $Q_L/(Q_L+Q_T)$ ratios.

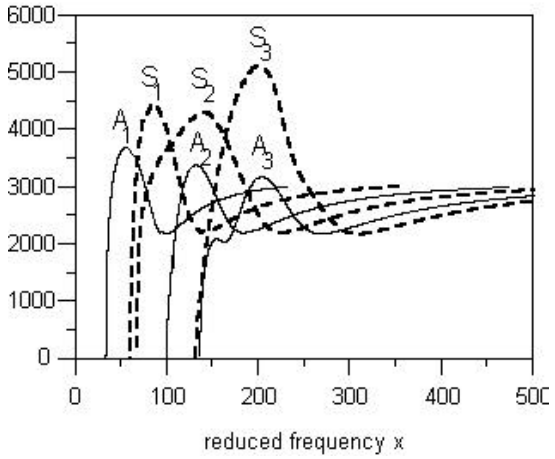

Figure 5: Evolutions of the energy velocities.

Conclusion

As for plane geometries, the use of frequency, angular, longitudinal and transverse quality factors is an interesting tool to investigate the Lamb-type waves propagating along a cylindrical shell. At our knowledge, there is no other methods which can give the polarization of the waves propagating along a cylindrical shell. Moreover, the energy velocity can also be obtained by means of the quality factors and for the waves studied, the group and energy velocities are shown to be equal.

Bibliographical references

[1] J. M. Conoir, J. L. Izbicki and O. Lenoir, *Phase Gradient Method applied to scattering by an elastic shell*, Ultrasonics, 157-169 (1996).
[2] **.** O. Lenoir, J. Duclos, J.M. Conoir and J.L. Izbicki, *Study of Lamb waves based upon the frequential and angular derivatives of the phase of the reflection coefficient,* J. Acoust. Soc. Am., **94**, 330-343 (1993).